RSC Advances

PAPER

View Article Online
View Journal | View Issue

Cite this: *RSC Adv.*, 2014, **4**, 3774

Cu(II) complex heterogenized on SBA-15: a highly efficient and additive-free solid catalyst for the homocoupling of alkynes

Anand Narani, Ravi Kumar Marella, Pochamoni Ramudu, Kamaraju Seetha Rama Rao and David Raju Burri*

Received 6th August 2013
Accepted 17th October 2013

DOI: 10.1039/c3ra44213f

www.rsc.org/advances

A Cu(II) complex has been heterogenized on SBA-15 by functionalization of SBA-15 with (*N*1-propylethane-1,2-diamine) triethoxysilane (NN-SBA-15) followed by anchoring of 2-pyridinecarboxaldehyde through Schiff's base formation between the terminal $-NH_2$ and the aldehyde group of 2-pyridinecarboxaldehyde (Py-NN-SBA-15), and finally, copper(II) was immobilized through complexation. Copper(II) complex heterogenized on SBA-15 (Cu(II)-SBA-15) has been thoroughly characterized by different techniques such as N_2 sorption, small-angle X-ray diffraction (XRD), thermogravimetric analysis (TGA), X-ray photoelectron spectroscopy (XPS), transmission electron microscopy (TEM) and solid-state ^{13}C CP-MAS NMR spectroscopy. Cu(II)-SBA-15 is an efficient heterogenized solid catalyst for the oxidative homocoupling of phenyl acetylene into 1,4-diphenylbuta-1,3-diyne with a yield of 97%, even in the absence of palladium, co-catalyst and base additives. In the case of the homocoupling of other aromatic and aliphatic terminal alkynes, the yields were 85–98%.

Introduction

Despite homogeneous catalysts being highly active for a variety of reactions, the problem of catalyst separation from the product mixture and the usage of large amounts of harmful solvents are the main obstacles to their wider industrial utility. Homogeneous catalysts are soluble salts or complexes of metals, whereas heterogeneous catalysts are insoluble robust materials. Hence, the separation of heterogeneous catalysts from the product mixture is facile, and furthermore these catalysts can be used in repeated cycles, thereby helping to minimize industrial waste. Consequently, the cost of the desired product can be significantly diminished. As a result of these significant advantages, the heterogenization of homogeneous catalysts on solid supports has been emerging as an important area of research in heterogeneous catalysis.[1]

Mesoporous catalytic supports are widely used due to their large surface area, controllable porosity, excellent stability, tuneable surface chemistry and good accessibility.[2] The primary advantage of using mesoporous supports is the minimization of diffusion limitations, even in the case of larger molecules. Hexagonally ordered mesoporous SBA-15 is a stable support compared to the M41S (MCM-41, MCM-48 and MCM-15) family and other members of the SBA (SBA-1, SBA-11, SBA-12, SBA-14 and SBA-16) family of mesoporous materials,[3] and in addition SBA-15 possesses a larger pore size. Due to its larger pore size and higher thermal and hydrothermal stability, SBA-15 has recently been garnering interest as a novel mesoporous support.

The direct attachment of catalytic centres to SBA-15 is a facile route to produce heterogeneous catalysts, but leaching of the active component into the reaction mixture is a serious problem from an industrial perspective. To avoid this problem, the grafting of catalyst by means of covalent linkage has been the subject of intensive investigation recently.[4] Furthermore, flexible organic linkages can provide greater accessibility to the catalytic centre by increasing the mobility of the loaded complex.[5] Organically functionalized mesoporous materials have the high capacity to immobilize metal ions, which is expected to limit the leaching of active metal from the support into the reaction mixture.

Conjugated 1,3-diyne derivatives are one of the most versatile building block materials, particularly in the fields of natural products,[6] pharmaceuticals,[7] polymers,[8] and medicinal chemistry, owing to their biological activities such as their anti-inflammatory, antifungal, anti-HIV, antibacterial, and anti-cancer activities *etc.*[9] The conjugated 1,3-diynes play an important role in the construction of macrocyclic annulenes,[10] organic conductors,[11] supramolecular switches[12] and carbon-rich materials.[13]

There are several methods available for the synthesis of 1,3-diynes. Glaser coupling is one of the conventional methods, in which oxidative homocoupling of two terminal alkynes takes place using Cu salts as catalyst to produce symmetrical 1,3-diynes.[14] 1,3-diynes can also be synthesized by Eglinton coupling,[15] Hay coupling,[16] and Sonagashira coupling *etc.*[17] The

Catalysis Laboratory, Indian Institute of Chemical Technology, Hyderabad-500007, India. E-mail: david@iict.res.in; Fax: +91-40-27160921; Tel: +91-40-27193232

commonly used catalytic systems are Pd,[18] Co,[19] and the combination of Cu and Ag[20] or Ni.[21] Highly active $(Ph_3P)_2PdCl_2$ and NHC–Pd(II) catalytic systems yielded 81% and 86% diyne, respectively, from phenyl acetylene in presence of CuI, Ph_3P, and CH_3CN/Et_3N. The requirement of poisonous phosphine, amine ligands and Cu mediated conditions is a drawback of Pd catalytic systems.[22] Alternatively, several groups have studied the homocoupling of alkynes using single copper salts. Wang *et al.* reported the oxidative homocoupling of terminal alkynes in the presence of $CuCl_2/Et_3N$ under solvent free conditions.[23] Kusuda *et al.* reported the homocoupling of terminal alkynes using CuCl/TMEDA catalyst in fluorinated solvents (Solkane@365mfc).[24] Successful methods are reported for the synthesis of 1,3-diynes using Cu(I) and Cu(II) salts without the addition of any Pd species, ligands or bases.[25] However, these copper-catalyzed homocoupling reactions are homogeneous. Hence, the separation of the catalyst from the reaction mixture, the reusability of the catalyst for subsequent reactions and the unacceptable copper contamination in the desired isolated product are the inherent disadvantages that need to be resolved. Recently, several copper-based heterogeneous catalytic systems for the oxidative homocoupling of terminal alkynes have been reported, such as Cu–Al hydrotalcite,[26] copper(I)-modified zeolites,[27] $Cu(OH)_x/TiO_2$,[28] copper nanoparticles,[29] CuI immobilized on MCM-41,[30] and polymer supported copper.[31] However, there are certain drawbacks to these catalytic systems such as the requirement of stabilizing ligands, addition of bases, high catalyst loading, high reaction temperature and low activity and selectivity.

Herein, the heterogenization of a homogeneous copper(II) complex on mesoporous SBA-15, its physio-chemical characterization and its catalytic application in the oxidative homocoupling of terminal alkynes into conjugated 1,3-diyne derivatives in the liquid phase without the use of any additives has been described.

Experimental procedures

Catalyst preparation

The synthesis of the parent silica SBA-15 has been described by Zhao *et al.*[32a] and in our own published procedures[32b,c] using P123 triblock co-polymer as a structure directing agent and tetraethylorthosilicate as a silica source under acidic and hydrothermal conditions. Finally, the template was removed from the as-made SBA-15 by a conventional calcination procedure and this template-free SBA-15 was used as a catalyst support.

The details of the catalyst preparation procedure are presented in Scheme 1. In a typical functionalization procedure, 3 g of template-free SBA-15 was degassed for 3 h at 150 °C under vacuum, and then dispersed in 50 ml of dry toluene under N_2 flow, before the addition of 3 mmol (*N*1-propylethane-1,2-diamine) triethoxysilane to the mixture which was then refluxed for 24 h. The solid product was recovered by filtration under vacuum, washed with 150 ml of toluene and dried at 100 °C in an air oven for 12 h and is designated as NN-SBA-15. In a typical anchoring of 2-pyridinecarboxaldehyde to NN-SBA-15, to 3 mmol of 2-pyridinecarboxaldehyde dissolved in absolute ethanol was added 1 g of NN-SBA-15 and the mixture was stirred for 18 h at room temperature. Later on, the material was filtered, washed with ethanol, dried under vacuum and the resultant material was designated as Py-NN-SBA-15. The vacuum dried Py-NN-SBA-15 was added to $Cu(OAc)_2$ in acetone solution, stirred at room temperature for 24 h and the catalyst paste was filtered off and washed thoroughly with acetone until the washings were colourless. The catalyst was dried overnight at 90 °C under vacuum and the material was designated as Cu(II)-SBA-15.

Catalyst characterization

Low-angle XRD patterns were recorded on an Ultima IV X-ray diffractometer at 40 kV and 40 mA using Cu Kα radiation in the range 0.7–5° at room temperature. X-ray photoelectron spectroscopy (XPS) analysis of the catalyst was carried out with a Kratos analytical spectrophotometer using Mg Kα monochromatic excited radiation (1253.6 eV). The residual pressure in the analysis chamber was around 10^{-9} mbar. The binding energy (BE) measurements were corrected for charging effects with reference to the C 1s peak of the adventitious carbon (284.6 eV). A Philips Tecnai F12 FEI transmission electron microscope (TEM) operating at 80–100 kV was used to record TEM images. The TGA measurements were carried out using a TGA/SDTA 851e thermal system (Mettler Toledo, Switzerland). The samples were heated in air from 27 to 1000 °C at a heating

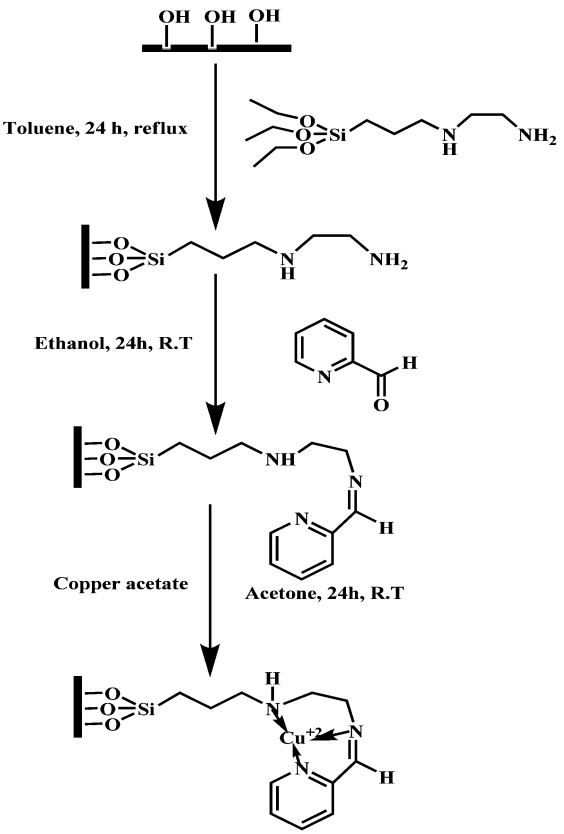

Scheme 1 Cu(II)-SBA-15 solid catalyst synthetic procedure.

Table 1 CHNS Elemental analysis and ICPMS for copper species[a]

Sample	Anal.	C %	H %	N %	S %	Cu^{2+} %
SBA-15	CHNS	NF	NF	NF	NF	—
NN-SBA-15	CHNS	11.6	1.96	3.8	NF	—
Py-NN-SBA-15	CHNS	14.3	2.90	4.6	NF	—
Cu(II)-SBA-15	ICPMS	—	—	—	—	2.75[b]
Cu(II)-SBA-15	ICPMS	—	—	—	—	2.73[c]

[a] NF stands for not found. [b] Fresh catalyst. [c] Used catalyst.

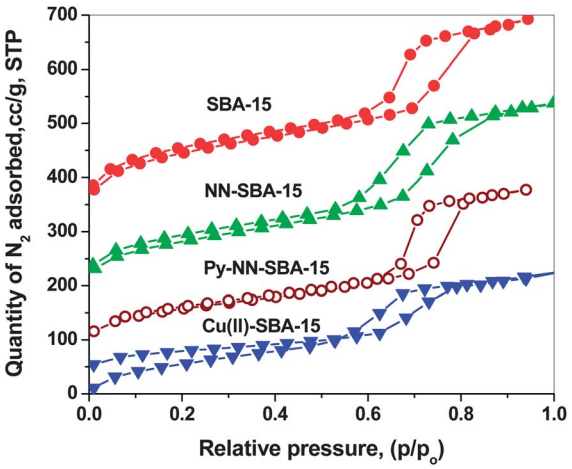

Fig. 1 N_2 adsorption–desorption isotherms of the different samples.

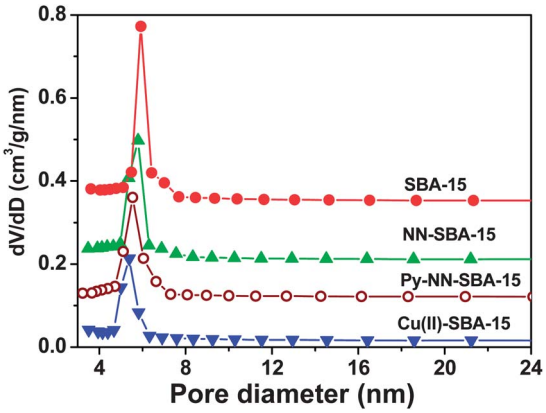

Fig. 2 Pore size distribution of the samples.

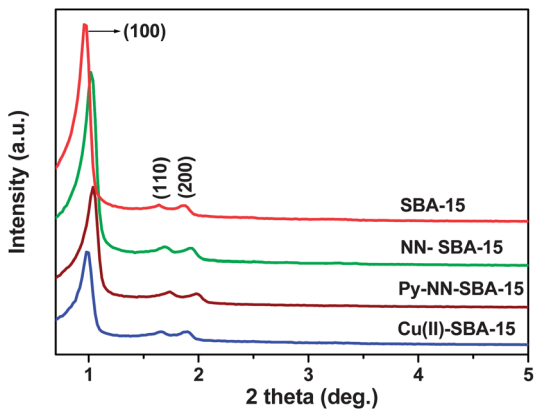

Fig. 3 Low-angle XRD patterns of the different samples.

rate of 10 °C min^{-1}. During the heating period, the weight loss and the temperature difference were recorded as a function of temperature. Solid-state ^{13}C CP-MAS NMR spectroscopy was obtained on a Bruker-Avance 500 MHz spectrometer with a 10 kHz spinning rate.

Catalyst activity test

All of the reactions were carried out in a 25 ml round bottom flask. In a typical experiment, 1 mmol of substrate was added to a mixture of 50 mg Cu(II)-SBA-15 catalyst and 3 ml solvent. The reaction mixture was stirred at 100 °C for a given reaction time. The progress of the reaction was monitored by TLC, and the reaction mixture was then cooled to room temperature and diluted with ethyl acetate followed by the separation of the catalyst from the reaction mixture by centrifugation. The crude residue was washed with brine solution, dried over anhydrous Na_2SO_4, and evaporated to obtain the crude product, which was purified by column chromatography to yield the desired product. The products were identified and analyzed using a GCMS-QP-5050 (M/s. Shimadzu Instruments, Japan) with a ZB-5 capillary column (25 m × 0.32 mm) supplied by M/s. J&W Scientific, USA. Toluene was used as an external standard for the quantification of the products.

Results and discussion

The loading of *N*1-propylethane-1,2-diamine and 2-pyridinecarboxaldehyde in NN-SBA-15 and Py-NN-SBA-15 were determined from carbon, hydrogen, nitrogen and sulphur (C,

Table 2 Structural and textural characteristics

Sample	S_{BET}[a] m^2 g^{-1}	V_p[b] cm^3 g^{-1}	D_p[c] nm	$d_{(100)}$[d] nm	a_o[e] nm	t_w[f] nm
SBA-15	789	1.12	7.15	9.09	10.5	4.59
NN-SBA-15	513	0.93	6.94	8.61	09.9	4.17
Py-NN-SBA-15	502	0.89	6.29	8.63	09.8	4.32
Cu(II)-SBA-15	485	0.81	6.03	8.92	10.3	4.92

[a] BET surface area. [b] Total pore volume. [c] Avg. pore diameter. [d] Spacing between two successive planes derived from low-angle XRD. [e] Unit cell length ($a_0 = 2d_{100}/\sqrt{3}$). [f] Pore wall thickness ($t_w = a_0 - D_{BJH}$).

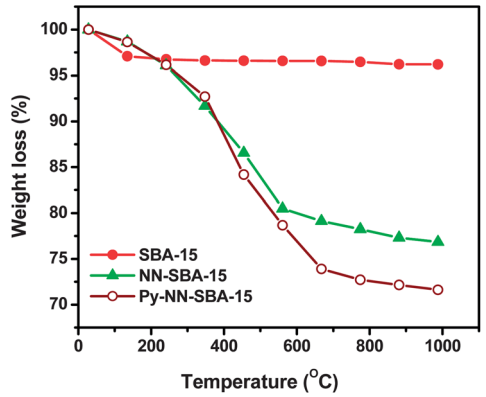

Fig. 4 Thermogravimetric analysis curves of the samples.

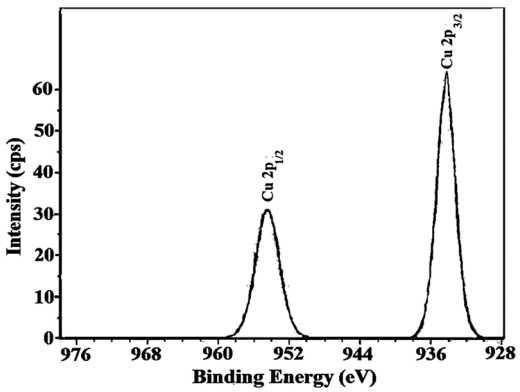

Fig. 5 X-ray photoelectron spectrum of the Cu(II)-SBA-15 catalyst.

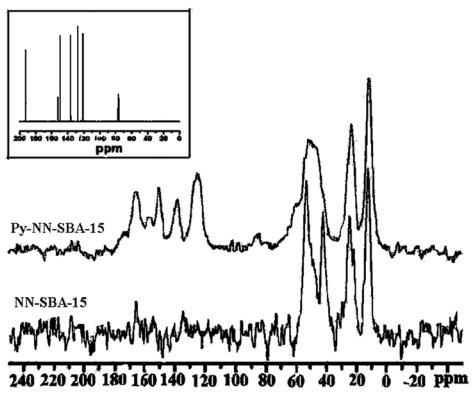

Fig. 6 ^{13}C CP-MAS NMR spectra of NN-SBA-15 and Py-NN-SBA-15.

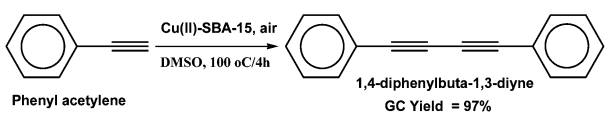

Scheme 2 Oxidative homocoupling of phenyl acetylene.

H, N and S) elemental analysis and the loading of copper in the Cu(II)-SBA-15 catalyst was determined by inductively coupled plasma mass spectrometry (ICPMS). The details of the analysis data are presented in Table 1, which reveals that the *N*1-propylethane-1,2-diamine loading is around 1.36 mmol g^{-1} and the 2-pyridinecarboxaldehyde loading is around 0.60 mmol g^{-1}. The loadings of Cu^{2+} metal ions in fresh and recycled catalysts were found to be 2.75 and 2.73 wt% respectively; from this data it is clear that there is no leaching of active metal during the course of the reaction.

The N_2 adsorption–desorption isotherms of the SBA-15, NN-SBA-15, Py-NN-SBA-15 and Cu(II)-SBA-15 catalysts are displayed in Fig. 1, which reveals that all of the catalysts exhibit a type IV

Table 3 Oxidative homocoupling of phenyl acetylene over different catalysts[a]

Entry	Catalyst	Time, h	Yield, %
1	SBA-15	4	No reaction
2	No catalyst	4	No reaction
3	CuO	4	Traces
4	$CuCl_2 \cdot H_2O$	4	15
5	$CuSO_4 \cdot 5H_2O$	4	37
6	$Cu(NO_3)_2 \cdot 3H_2O$	4	12
7	$Cu(acac)_2$	4	18
8	Cu(II)-SBA-15	4	97

[a] Phenyl acetylene = 1 mmol, DMSO = 3 ml, catalyst = 50 mg, temperature = 100 °C.

Table 4 Effect of solvent on Cu(II)-SBA-15[a]

Entry	Solvent	Yield, %
1	DMSO	97
2	CH_3CN	52
3	DCE	45
4	DCM	57
5	DMF	79
6	CH_3OH	68
7	Benzene	23
8	Toluene	15
9	H_2O	Traces

[a] Catalyst: 50 mg, phenyl acetylene: 1 mmol, solvent: 3 ml, temperature: 100 °C, pressure: 1 atm, time: 4 h.

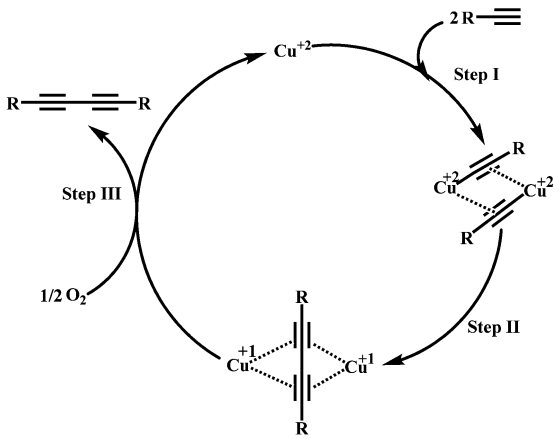

Scheme 3 Proposed reaction mechanism for the homocoupling of alkynes to 1,3-diynes over the Cu(II)-SBA-15 solid catalyst.

Table 5 Oxidative homocoupling activity of Cu(II)-SBA-15 on different acetylene substrates[a]

Entry	Reactant	Product	Time, h	Yield, %	TOF (h^{-1})
1			4	97	11.4
2			3	97	15
3	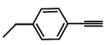		2.5	98	18.4
4	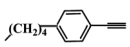		3	96	15
5			4	89	10.4
6			1.5	92	28.2
7	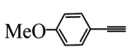		2.5	98	18.4
8		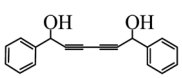	3.5	65	8.5
9		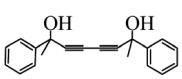	2	98	23
10	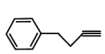	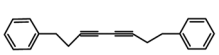	1.5	96	30.1
11		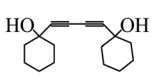	1.5	97	30
12			1	98	46.1
13		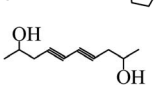	2.5	72	22.6
14	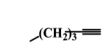		1.1	85	33
15		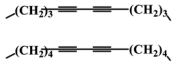	1	87	41
16	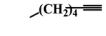		1	90	42.3
17	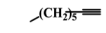		0.9	91	47
18	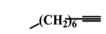		0.9	93	48.5

[a] Substrate = 1 mmol, DMSO = 3 ml, catalyst = 50 mg, temperature = 100 °C.

adsorption isotherm with an H1 hysteresis loop, which is a characteristic property of ordered mesoporous materials.[33] The BET surface area, total pore volume, average pore diameter and pore wall thickness are shown in Table 2. Due to sequential attachment of organic spacers/linkers on the pore wall, an increase in pore wall thickness might have occurred. The diminishing of the surface area, pore volume, and pore diameter in each step of the catalyst preparation is due to the introduction of *N*1-propylethane-1,2-diamine, 2-pyridinecarboxaldehyde and the subsequent coordination of Cu^{2+} metal ions. This diminishing trend indicates the partial blockage of certain mesopores with the functionalizing agents and the Cu^{2+} metal complex. Indeed, the presence of some amount of copper species in the pore wall may not be ruled out.

The pore size distribution curves are shown in Fig. 2. The pores are narrowly distributed in the range of 4.4–7.8 nm, which reveals the existence of ordered mesopores.

The small-angle XRD pattern of parent SBA-15, NN-SBA-15, Py-NN-SBA-15 and Cu(II)-SBA-15 are shown in Fig. 3. The parent SBA-15 shows three strong diffraction peaks at 0.97, 1.63 and 1.86° on the 2 theta scale, which are assigned to the (100), (110) and (200) planes of 2D-hexagonal mesophase indicating the formation of ordered mesoporous SBA-15. The NN-SBA-15, Py-NN-SBA-15 and Cu(II)-SBA-15 samples show similar diffraction patterns, which indicates the retention of the 2D-hexagonal mesoporous structure after anchoring with *N*1-propylethane-1,2-diamine, 2-pyridinecarboxaldehyde and the coordination of Cu^{2+} metal ions. The grafting procedure did not significantly diminish the ordered mesoporous structure of SBA-15 but there is a small shift in the 2 theta and a decrease in the signal intensities, which could be attributed to the lowering of the local order. This particular decrease in local order may be due to reduction of scattering contrast between the channels of the SBA-15 frame work and the functionalized moieties partially filling the pores.[34]

Fig. 4 shows the thermogravimetric analysis curves of SBA-15, NN-SBA-15, Py-NN-SBA-15 and Cu(II)-SBA-15. For the parent SBA-15, a marginal 2.91% weight loss is observed. This is mainly

due to the loss of adsorbed water from the surface of SBA-15, or the water that formed from the condensation of hydroxyl groups. The weight losses observed for the NN-SBA-15 and Py-NN-SBA-15 anchored samples are at two temperatures; the minor weight loss is observed between 90–130 °C, which is due to physically adsorbed water molecules on the surface of the SBA-15. The major weight loss between 345–650 °C is due to the thermal decomposition of grafted *N*1-propylethane-1,2-diamine and 2-pyridinecarboxaldehyde moieties. Beyond this temperature, the weight loss is more or less constant. The TGA curves demonstrate the covalent anchoring of organic moieties on to the surface of SBA-15.

The XPS spectrum of the Cu(II)-SBA-15 catalyst is depicted in Fig. 5. The 934.32 and 954.49 eV binding energies correspond to spin orbit splitting components of Cu $2p_{3/2}$ and Cu $2p_{1/2}$ in the +2 oxidation state of copper, which are in agreement with the reported literature values.[35] Based on the XPS results, the Cu species in the Cu(II)-SBA-15 catalyst is found to be in the +2 oxidation state.

The ^{13}C CP-MAS NMR study provides useful information regarding the presence of organic moieties present in the material. The anchoring of *N*1-propylethane-1,2-diamine and subsequently 2-pyridinecarboxaldehyde to SBA-15 has been confirmed by solid state ^{13}C NMR spectroscopy. Fig. 6 shows the solid-state NMR spectra of NN-SBA-15 and Py-NN-SBA-15. The ^{13}C NMR spectrum of NN-SBA-15 shows five signals at 12.63, 22.21, 24.76, 42.39 and 53.42 ppm, representing C^1, C^2, C^3, C^4 and C^5 of the N^1-(3-(triethoxysilyl)propyl)ethane-1,2-diamine, which confirms the *N*1-propylethane-1,2-diamine functionalization on the surface of SBA-15. The single peak that appears at 192.8 ppm for the pure 2-pyridinecarboxaldehyde corresponds to –C═O of –COH. (Fig. 6, inset). After 2-pyridinecarboxaldehyde was used to treat NN-SBA-15, the peak at 192.8 ppm of pure 2-pyridinecarboxaldehyde disappeared and a new peak was observed at 165.4 ppm, indicating the imine (–C═N) formation through the Schiff's base condensation between the $–NH_2$ and –C═O groups. Additionally, the ^{13}C NMR spectrum of Py-NN-SBA-15 shows peaks at 157.3, 150.54, 138.04, 125.03, 121.08 ppm, which confirms the formation of the imine (–C═N) bond.

In order to evaluate the present Cu(II)-SBA-15 catalyst for the oxidative homocoupling of acetylenes into respective 1,3-diynes, phenyl acetylene homocoupling has been taken as a model reaction. As shown in Scheme 2, the homocoupling of phenyl acetylene proceeded well over Cu(II)-SBA-15 in DMSO solvent under air at 100 °C for 4 h. Under these reaction conditions, the yield of 1,4-diphenylbuta-1,3-diyne is about 97% (entry 8 of Table 3). The results demonstrate that the Cu(II)-SBA-15 is a highly efficient heterogenized solid catalyst for the homocoupling of phenyl acetylene into 1,4-diphenybuta-1,3-diyne. The catalytic activity of Cu(II)-SBA-15 is relatively comparable with the reported highly active homogeneous catalysts such as homogeneous $Cu(OAc)_2H_2O$ catalyst, which produced 1,4-diphenybuta-1,3-diyne with a yield of about 90% at 90 °C in 10 h,[25b] a homogeneous CuCl catalyst for the homocoupling of phenyl acetylene to 1,3-diyne (yield, 93%) at room temperature with TMEDA base and Solkane@365mfc solvent in 1 h (ref. 24) and a homogeneous CuCl catalyst using piperidine as a base and toluene as a solvent, produced 1,3-diyne in 96% yield.[36] Few heterogeneous catalysts with high homocoupling activities in the presence of suitable bases are reported. For example, CuI catalyst immobilized on MCM-41 and polymer supported CuI catalyst effectively converted phenyl acetylene into 1,3-diyne with yields of 94 and 97% respectively, in the presence of different base additives.[30,31] Cu nanoparticles supported on TiO_2 is one of the best catalysts, which effectively produced 1,3-diyne in 99% yield in the presence of piperidine base.[29b]

The high activity of the Cu(II)-SBA-15 solid catalyst can be ascribed to its hexagonally ordered arrangement of mesopores, in which the covalently anchored active Cu^{2+} species are readily accessible to the reactants for their adsorption, surface reaction and desorption of products without any diffusion limitations. In other words, the hexagonally arranged mesopores containing the reactive Cu^{2+} species act as a multi-tubular reactor.

To compare the catalytic performance of the Cu(II)-SBA-15 catalyst, different copper salts were used under optimized reaction conditions and the results are summarized in Table 3. The reaction did not proceed in the absence of catalyst. Similarly the reaction did not occur with SBA-15 alone (Table 3, entries 1and 2). When the CuO was used as a catalyst no significant activity was observed. All of the homogeneous catalysts (Table 3, entries 4–7) exhibited moderate activity.

To identify a suitable solvent, the selected model reaction was carried out in different solvents under identical conditions and the results are summarized in Table 4, which reveals that DMF and DMSO solvents gave good to excellent yields of the desired product (Table 4, entries 1 and 5), while DCE, CH_2Cl_2, CH_3CN and CH_3OH gave moderate yields (Table 4, entries 3, 4, 2 and 6). The yields were negligible when benzene and toluene were used. The yield of the desired product was negligible when H_2O was used as a solvent. According to Mizuno *et al.*[37c] the yields of diyne are 86% and 90% in DMSO and DMF solvents respectively, using molecular sieves MS (4A, 200 mg) over a di-copper-substituted silicotungstate homogeneous catalyst. Whereas with non-polar and polar protic solvents, lower yields of diyne were obtained. With DMSO solvent the yield of diyne was 90% over $Cu(OAc)_2$ homogeneous catalyst at 90 °C.[25b] Indeed, the solvents play a crucial role on the efficiency of these Cu(II) catalytic systems. Through some interaction, polar aprotic solvents like DMSO and DMF favour the activity of homogeneous Cu(II) catalysts and Cu(II)-SBA-15 heterogeneous catalyst for the alkyne homocoupling. The significant advantage of the Cu(II)-SBA-15 catalyst is its heterogeneous nature and high activity in DMF and DMSO solvents, even in the absence of any additives.

On the basis of the present results and the literature reports,[37] a possible reaction mechanism is proposed for the oxidative homocoupling of terminal alkynes into 1,3-diyne derivatives over the Cu(II)-SBA-15 catalyst, which is shown in Scheme 3. In the initial step, the formation of a di-copper(II)-alkynyl intermediate $\{Cu_2(\mu\text{-}CCR)_2\}$ takes place by the reaction of Cu^{2+} with 2 moles of terminal alkynes, which readily reduced to a Cu^{1+} species in step II. In step III, the desired diyne product formation and re-oxidation of the reduced Cu^{1+} species into Cu^{2+} occurs simultaneously *via* the O_2 supplied during the reaction.

Under optimized reaction conditions, the homocoupling of various terminal alkynes including aliphatic and aromatic terminal alkynes with different functional groups were examined to investigate the substrate scope of the reaction, and the results are summarized in Table 5, wherein, good to excellent yields of 1,3-diynes were obtained.

The oxidative homocoupling of phenyl acetylenes which contain electron donating (methyl, ethyl, *n*-pentyl, –oxymethyl) as well as electron withdrawing groups (–F, –Cl) proceeded smoothly to afford the corresponding diyne derivatives in 89–98% yields (Table 5, entries 2, 3, 4 and 7). In the case of –OH substituted terminal alkynes, when the –OH group is in the tertiary position, the yields of the corresponding diynes are higher (Table 5, entries 9 and 11) compared to those with the –OH group present in the secondary position (Table 5, entries 8 and 13), which is due to the oxidation of alcohol to ketones. The homocoupling reaction of aliphatic terminal alkynes proceeded more rapidly than that of aromatic terminal alkynes (Table 5, entries 14–18).

Conclusions

Cu(II)-SBA-15 catalyzed the oxidative homocoupling of terminal alkynes into the corresponding conjugated 1,3-diyne derivatives up to 98% yields, even in absence of additives and/or bases. The high activity (85–98% yields) of this solid catalyst may be endowed by the isolated distribution of Cu(II) complexes, their coordination environment, ease of accessibility and the confined mesoporous environment of hexagonally ordered mesopores of the SBA-15 support.

Acknowledgements

Anand, Ravi Kumar and Ramudu acknowledge the Council of Scientific and Industrial Research (CSIR), New Delhi for the award of research fellowships.

Notes and references

1 L. Canali and D. C. Sherrington, *Chem. Soc. Rev.*, 1999, **28**, 85; M.-C. Hsiao and S.-T. Liu, *Catal. Lett.*, 2010, **139**, 61; S. Minakata and M. Komatsu, *Chem. Rev.*, 2009, **109**, 711; *Supported Catalysts and Their Applications*, ed. D. C. Sherrington and A. P. Kybett, RSC, Cambridge, 2001; D. R. Burri, K.-W. Jun, Y.-H. Kim, J. M. Kim, S.-E. Park and J. S. Yoo, *Chem. Lett.*, 2002, 212; D. R. Burri, R. S. Isak, K. M. Choi and S.-E. Park, *Catal. Commun.*, 2007, **8**, 731; N. Anand, K. H. P. Reddy, V. Swapna, K. S. Rama Rao and D. R. Burri, *Microporous Mesoporous Mater.*, 2011, **143**, 132; N. Anand, K. H. P. Reddy, K. S. Rama Rao and D. R. Burri, *Catal. Lett.*, 2011, **141**, 1355.

2 L. Yin and J. Liebscher, *Chem. Rev.*, 2007, **107**, 133.

3 V. Meynen, P. Cool and E. F. Vansant, *Microporous Mesoporous Mater.*, 2009, **125**, 170.

4 D. Choudhary, S. Paul, R. Gupta and J. H. Clark, *Green Chem.*, 2006, **8**, 479.

5 B. Karimi, A. Zamani and J. H. Clark, *Organometallics*, 2005, **24**, 4695.

6 A. L. K. Shi Shun and R. R. Tykwinski, *Angew. Chem., Int. Ed.*, 2006, **45**, 1034.

7 A. Stutz and G. Petranyi, *J. Med. Chem.*, 1984, **27**, 1539; A. Stutz, *Angew. Chem., Int. Ed. Engl.*, 1987, **26**, 320.

8 J. M. Tour, *Chem. Rev.*, 1996, **96**, 537; R. E. Martin and F. Diederich, *Angew. Chem., Int. Ed.*, 1999, **38**, 1350.

9 M. L. Lerch, M. K. Harper and D. J. Faulkner, *J. Nat. Prod.*, 2003, **66**, 667; D. Lechner, M. Stavri, M. Oluwatuyi, R. Perda-Miranda and S. Gibbons, *Phytochemistry*, 2004, **65**, 331.

10 M. Gholami and R. R. Tykwinski, *Chem. Rev.*, 2006, **106**, 4997; J. A. Marsden and M. M. Haley, *J. Org. Chem.*, 2005, **70**, 10213.

11 *Polyynes: Synthesis Properties, and Applications*, ed. F. Cataldo, CRC Press/Taylor & Francis, Boca Raton, Florida, 2005.

12 J. D. Crowley, S. M. Goldup, A. L. Lee, D. A. Leigh and R. T. McBurney, *Chem. Soc. Rev.*, 2009, **38**, 1530.

13 F. Diederich, P. J. Stang and R. R. Tykwinski, *Acetylene Chemistry:Chemistry, Biology and Material Science*, Wiley-VCH Verlag GmbH & Co. KGaA, Weinheim, Germany, 2005.

14 C. Glaser, *Ber. Dtsch. Chem. Ges.*, 1869, **2**, 422; J. Li and H. Jiang, *Chem. Commun.*, 1999, 2369; J. S. Yadav, B. V. S. Reddy, K. B. Reddy, K. U. Gayathri and A. R. Prasad, *Tetrahedron Lett.*, 2003, **44**, 6493.

15 K. Inouchi, S. Kabashi, K. Takimiya, Y. Aso and T. Otsubo, *Org. Lett.*, 2002, **4**, 2533.

16 A. S. Hay, *J. Org. Chem.*, 1960, **25**, 1275; A. S. Hay, *J. Org. Chem.*, 1962, **27**, 3320.

17 K. Sonogashira, Y. Tohda and N. Hagihara, *Tetrahedron Lett.*, 1975, **16**, 4467.

18 A. S. Batsanov, J. C. Collings, I. J. S. Fairlamb, J. P. Holland, J. A. K. Howard, Z. Y.Lin, T. B. Marder, A. C. Parsons, R. M. Ward and J. Zhu, *J. Org. Chem.*, 2005, **70**, 703; M. Shi and H. X. Qian, *Appl. Organomet. Chem.*, 2006, **20**, 771.

19 M. E. Krafft, C. Hirosawa, N. Dalal, C. Ramsey and A. Stiegman, *Tetrahedron Lett.*, 2001, **42**, 7733; G. Hilt, C. Hengst and M. Arndt, *Synthesis*, 2009, 395.

20 Y. Liao, R. Fathi and Z. Yang, *Org. Lett.*, 2003, **5**, 902.

21 W. Y. Yin, C. He, M. Chen, H. Zhang and A. W. Lei, *Org. Lett.*, 2009, **11**, 709; J. D. Crowley, S. M. Goldup, N. D. Gowans, D. A. Leigh, V. E. Ronaldson and A. M. Z. Slawin, *J. Am. Chem. Soc.*, 2010, **132**, 6243.

22 P. Kuhn, A. Alix, M. Kumarraja, B. Louis, P. Pale and J. Sommer, *Eur. J. Org. Chem.*, 2009, 423; T. Oishi, T. Katayama, K. Yamaguchi and N. Mizuno, *Chem.–Eur. J.*, 2009, **15**, 7539; S. Chassaing, A. Alix, T. Boningari, K. S. S. Sido, M. Keller, P. Kuhn, B. Louis, J. Sommer and P. Pale, *Synthesis*, 2010, 1557.

23 D. Wang, J. Li, N. Li, T. Gao, S. Hou and B. Chen, *Green Chem.*, 2010, **12**, 45.

24 A. Kusuda, X.-H. Xu, X. Wang, E. Tokunaga and N. Shibata, *Green Chem.*, 2011, **13**, 843.

25 (*a*) K. Yin, C. J. Li, J. Li and X. S. Jia, *Green Chem.*, 2011, **13**, 591; (*b*) X. Jia, K. Yin, C. Li, J. Li and H. Bian, *Green Chem.*, 2011, **13**, 2175.
26 B. C. Zhu and X. Z. Jiang, *Appl. Organomet. Chem.*, 2007, **21**, 345.
27 P. Kuhn, A. Alix, M. Kumarraja, B. Louis, P. Pale and J. Sommer, *Eur. J. Org. Chem.*, 2009, 423.
28 T. Oishi, T. Katayama, K. Yamaguchi and N. Mizuno, *Chem.–Eur. J.*, 2009, **15**, 7539.
29 (*a*) F. Nador, L. Fortunato, Y. Moglic, C. Vitale and G. Radivoy, *Synthesis*, 2009, 4027; (*b*) F. Alonso, T. Melkonian, Y. Moglie and M. Yus, *Eur. J. Org. Chem.*, 2011, 2524.
30 R. Xiao, R. Yao and M. Cai, *Eur. J. Org. Chem.*, 2012, 4178.
31 Y. He and C. Cai, *Catal. Sci. Technol.*, 2012, **2**, 1126.
32 (*a*) D. Zhao, J. Feng, Q. Huo, N. Melosh, G. H. Fredrickson, B. F. Chemika and G. D. Stucky, *Science*, 1998, **279**, 548; (*b*) S. Ganji, P. Bukiya, V. Vakati, K. S. R. Rao and D. R. Burri, *Catal. Sci. Technol.*, 2013, **3**, 409; (*c*) S. Ganji, S. Mutyala, C. K. Neeli, K. S. Rama Rao and D. R. Burri, *RSC Adv.*, 2013, **3**, 11533.
33 S. J. Gregg and K. S. W. Sing, *Adsorption, Surface Area and Porosity*, Academic Press, London, 1982.
34 M. H. Limand and A. Stein, *Chem. Mater.*, 1999, **11**, 3285.
35 C. K. Prasad Neeli, A. Narani, R. K. Marella, K. S. Rama Rao and D. R. Burri, *Catal. Commun.*, 2013, **39**, 5.
36 Q. Zheng, R. Hua and Y. Wan, *Appl. Organomet. Chem.*, 2010, **24**, 314.
37 (*a*) P. Siemsen, R. C. Livingston and F. Diederich, *Angew. Chem., Int. Ed.*, 2000, **39**, 2632; (*b*) F. Bohlmann, H. Schönowsky, E. Inhoffen and G. Grau, *Chem. Ber.*, 1964, **97**, 794; (*c*) N. Mizuno, K. Kamata, Y. Nakagawa, T. Oishi and K. Yamaguchia, *Catal. Today*, 2010, **157**, 359.